Supporting Information

Aylett and Löwe 10.1073/pnas.1210899109

SI Materials and Methods

Sources. Unless stated, chromatography equipment was provided by GE Healthcare, chemicals by Sigma Aldrich, oligonucleotides by IDT, crystallography consumables by Hampton Research, and molecular graphics generated using PyMol (Schrödinger).

DNA, Genes, and Vectors. The genes encoding *Bacillus thuringiensis* serovar *israelensis* (ATCC; 35646) pBtoxis TubR and TubZ (UniProt Q8KNP2 and -3) were cloned directly from the species' DNA, kindly provided by R. A. Larsen and J. Pogliano (University of California, San Diego). The gene encoding *Bacillus megaterium* (ATCC 12872) pBM400 TubR (UniProt Q848W2) was synthesized, codon optimized (GenScript). Both expression vectors were based upon pHis17 (1). Construct pHis17–*Bt-tubR* encoded the complete sequence of *Bt* TubR and construct pHis17–*Bm-tubR* encoded the complete codon optimized sequence of *Bm* TubR. Constructs pHis17–*Bt-tubR*–His_6 and pET28–*Bt-tubZ*–His_6, adding six histidine residues at the C termini were also generated. These constructs were used solely for the microarray and light scattering experiments; no changes were made to the published sequence of either protein. The DNA sequence for *Bt tubC*24 was TTTAAGTTTAACTTTCAGTTTACA and its complement. Full-length *Bt tubC* was represented by a PCR product encompassing base pairs 126510–126649 of pBtoxis, repeats 1–3 by 126607–126654, and repeats 4–7 by 126526–126573, whereas the pBM400 intergenic region was represented by 44230–44369. Plasmid p*tubC* consisted of full-length *Bt tubC* product cloned into pHis17.

DNA Microarray. A DNA microarray was produced that consisted of 24-bp double-stranded variable sequences as 60-bp hairpins capped using a tetraloop sequence and scanned through the region of pBtoxis between base pairs 122000 and 3100 by 4-bp increments, and the region around *tubZR* (between base pairs 126787 and 126451) by 1-bp increments. This experiment was carried out through the aptamer microarray service at LC Sciences, Houston. Briefly, 0.2 μg/mL *Bt* TubR–His_6 was applied to the microarray in 100 mM Tris·Cl 8.5, 100 mM NaCl, 1 mM EDTA, 1% (wt/vol) BSA at 30 °C for 2 h. The chip was then washed with the same buffer without protein, and Alexa-647 labeled antihexahistidine antibody applied to the chip in the same fashion as protein for 1 h. The chip was washed once more and then scanned at 635 nm. The discrete Fourier coefficient for each whole number of base pairs was calculated and subsequently plotted against the base pair repeat as shown in Fig. S1.

Electrophoretic Mobility Shift Assays. The indicated PCR products were produced from primers 5′ conjugated to fluorescein. DNA was purified by gel extraction and then incubated with the indicated concentrations of *Bt* or *Bm* TubR in a final volume of 10 μL standard TBE buffer supplemented with 0.1 mg/mL BSA and 5% (vol/vol) glycerol for 30 min at 25 °C. Protein–DNA complexes were separated by native PAGE using Criterion 4–20% TBE gels according to the manufacturer's instructions (BioRad). The fluorescein-labeled DNA was detected using a Typhoon Trio imager (GE Healthcare) using the manufacturer's recommended standard sensitivity settings for fluorescein.

Light Scattering (90°). Light scattering experiments were performed using a Perkin-Elmer LS55 luminescence spectrometer in 25 mM Tris·Cl pH 8.0, 100 mM KCl, 2 mM $MgCl_2$, 0.5 mM EDTA at 20 °C with constant stirring of the 1-mL quartz cuvettete. Excitation and emission wavelengths were held at 400 nm, and the photon multiplier set to 650 V. TubZ was added to a final concentration of 1.25 μM, whereas 250 μM nucleotide was added at the indicated time point. *Bt* TubR was added to a final concentration of 500 nM when indicated, and the concentration of identified TubR binding sites within the DNA added was held constant at 125 nM, except in the case of *Bt tubC* with four TubR binding sites (sites 4–7), where this concentration was doubled to allow the effect upon polymerization to be clearly visible for the benefit of the reader.

Electron Microscopy. *Bt* or *Bm* TubR (10 mg/mL) and 100 μM of a 150-bp PCR product containing *Bt tubC* or the *Bm* intergenic region were diluted 2,000-fold into 25 mM Na-Hepes pH 7.5, 50 mM KCl, 1 mM $MgCl_2$. Samples were applied to carbon-coated Cu/Rh 300 mesh grids (Agar Scientific). The grids were blotted and stained with 0.5% (wt/vol) uranyl formate. Images were recorded to film (Kodak Electron; 1 s) or CCD (TVIPS; F214) using a Tecnai T12 electron microscope (FEI) at 120 kV, −2 to −6 μm defocus.

Rotary Shadowing. Before shadowing, *Bt* TubR*C* was diluted into 100 mM ammonium hydrogencarbonate, 50% (vol/vol) glycerol, giving a final concentration of 0.1 mg/mL. The sample was applied to carbon-coated grids, dried under high vacuum for 4 h, and then shadowed. Rotary shadowing was performed with an Edwards E306A coating system using a molten platinum source at an oblique angle of 3° and at a sample-to-source distance of 10 cm.

Protein Expression. C41 *E. coli* (Invitrogen) carrying the requisite expression vector were grown in 12 L 2xYT broth or M9 media, for selenomethionine (Acros Organics) substituted protein, according to the protocol of van den Ent and colleagues (2). Cultures were supplemented with 100 μg/L ampicillin or 50 μg/L kanamycin as appropriate and grown at 37 °C. Expression was induced by addition of isopropyl-β-D-1-thiogalactopyranoside to a final concentration of 1 mM, at an optical density at 600 nm of 1.0, and cells were harvested by centrifugation at 4 × *g* after 18 h expression at 20 °C.

Protein Purification. The pellet yielded by 1 L bacterial culture was resuspended in 20 mL 100 mM Na-Hepes pH 7.0 and broken at 25 kpsi, 4 °C using a cell disruption system (Constant Systems). Protein was then purified by chromatography from the supernatant after centrifugation at 45,000 × *g*. TubR proteins were retrieved by heparin affinity chromatography (5 mL HiTrap heparin HP, 25 mM Na-Hepes pH 7.0, 0–1 M NaCl), followed by purification by ion exchange (5 mL HiTrap Q HP, 25 mM Tris·Cl pH 8.5, 0.1–0.5 M NaCl) and size exclusion chromatography (HiLoad Sephacryl S200 16/60, 25 mM Tris·Cl pH 8.5, 0.1 M NaCl, 1 mM EDTA, 1 mM NaN_3). Protein was concentrated to 10 mg/mL before and after size exclusion chromatography in 20 mL, 10-kDa cutoff centrifugal concentrators (Vivaspin). TubZ protein was retrieved by nickel affinity chromatography (HisTrap HP, Tris·Cl pH 8.5, 0–1 M imidazole gradient), and crystallographic purity achieved by ion exchange (HiTrap Q HP, Tris·Cl pH 8.5, 100–500 mM NaCl gradient) followed by size exclusion chromatography (HiLoad Sephacryl S200 16/60, Tris·Cl pH 8.5, 150 mM NaCl, 1mM EDTA, 1mM NaN_3).

Crystallization. Initial conditions were identified using the high-throughput Medical Research Council Laboratory of Molecular Biology (MRC-LMB) crystallization facility (3). *Bt* TubR–*tubC* crystals were produced in 500 nL to 500 nL protein to precipitant drops: 10 mg/mL *Bt* TubR, 500 μM *tubC*24 or -26, 100 mM Na-

Hepes pH 7.5, 5 mM $MgCl_2$, 25% (wt/vol) polyacrylic acid 5100 sodium salt. Artificial mother liquor supplemented to 25% (vol/vol) glycerol was used as a cryoprotectant. *Bm* TubR crystals were produced in 500 nL to 500 nL protein to precipitant sitting drops: 20 mg/mL *Bm* TubR, 100 mM Tris·Cl pH 8.5, 0.2 M sodium citrate, 15% (vol/vol) PEG 400. Artificial mother liquor supplemented to 30% (vol/vol) PEG 400 was used as a cryoprotectant.

Crystallography. Diffraction images of *Bm* TubR and *Bt* TubR–*tubC*24 crystals were collected at European Synchrotron Research Facility beamline ID29 and Diamond beamline I03. Diffraction images were processed with XDS (4), POINTLESS (5), and SCALA (6). Initial phases for *Bm* TubR were determined by single wavelength anomalous dispersion (SAD). The Se substructure was solved with SHELXCDE (7) and phases were calculated with PHASER (8). The model was built manually with MAIN (9) and refined with REFMAC5 (10) and PHENIX (11). Initial phases for both *Bt* TubR–*tubC* crystal structure were determined by molecular replacement using PHASER (8) with ideal B-form DNA from Web3DNA (12) and Protein Data Bank (PDB) ID code 3M8E as search models. The models were refined as rigid bodies using PHENIX, the DNA being split into 12-bp double-stranded sections to allow for distortion. Selenium SAD anomalous differences were reserved for validation, the calculated phases from refinement being used to phase the anomalous differences. Anomalous scattering peaks were visible at the sites occupied by the selenium atoms of the selenomethionine residues, validating the structure independently (Fig. S3).

Structural Calculations. Structural superimpositions and alignments were carried out using the DALI-lite webserver (13). The output *Z*-score for PDB ID codes 3M9A and 4ASN was 10.9 and the rmsd, 2.0 Å. Surface area calculations were performed using the PDBe-PISA webserver and PDB ID codes 4ASN and 4ASO (14).

1. Miroux B, Walker JE (1996) Over-production of proteins in *Escherichia coli*: Mutant hosts that allow synthesis of some membrane proteins and globular proteins at high levels. *J Mol Biol* 260:289–298.
2. van den Ent F, Lockhart A, Kendrick-Jones J, Löwe J (1999) Crystal structure of the N-terminal domain of MukB: A protein involved in chromosome partitioning. *Structure* 7:1181–1187.
3. Stock D, Perisic O, Löwe J (2005) Robotic nanolitre protein crystallisation at the MRC Laboratory of Molecular Biology. *Prog Biophys Mol Biol* 88:311–327.
4. Kabsch W (2010) XDS. *Acta Crystallogr D Biol Crystallogr* 66:125–132.
5. Evans P (2006) Scaling and assessment of data quality. *Acta Crystallogr D Biol Crystallogr* 62:72–82.
6. Collaborative Computational Project, Number 4 (1994) The CCP4 suite: Programs for protein crystallography. *Acta Crystallogr D Biol Crystallogr* 50:760–763.
7. Sheldrick GM (2008) A short history of SHELX. *Acta Crystallogr A* 64:112–122.
8. McCoy AJ, et al. (2007) Phaser crystallographic software. *J Appl Cryst* 40:658–674.
9. Turk D (1992) Weiterentwicklung eines Programms für Molekülgraphik und Elektronendichte-Manipulation und seine Anwendung auf verschiedene Protein Strukturaufklärungen [Improvement of a computer program for molecular graphics and electron density manipulations and its application for various protein structure determinations] (PhD thesis, Technical University of Munich, Germany).
10. Murshudov GN, Vagin AA, Dodson EJ (1997) Refinement of macromolecular structures by the maximum-likelihood method. *Acta Crystallogr D Biol Crystallogr* 53:240–255.
11. Adams PD, et al. (2010) PHENIX: A comprehensive Python-based system for macromolecular structure solution. *Acta Crystallogr D Biol Crystallogr* 66:213–221.
12. Zheng G, Lu X-J, Olson WK (2009) Web 3DNA—a web server for the analysis, reconstruction, and visualization of three-dimensional nucleic-acid structures. *Nucleic Acids Res* 37(Web Server issue):W240-6.
13. Holm L, Park J (2000) DaliLite workbench for protein structure comparison. *Bioinformatics* 16:566–567.
14. Krissinel E, Henrick K (2007) Inference of macromolecular assemblies from crystalline state. *J Mol Biol* 372:774–797.

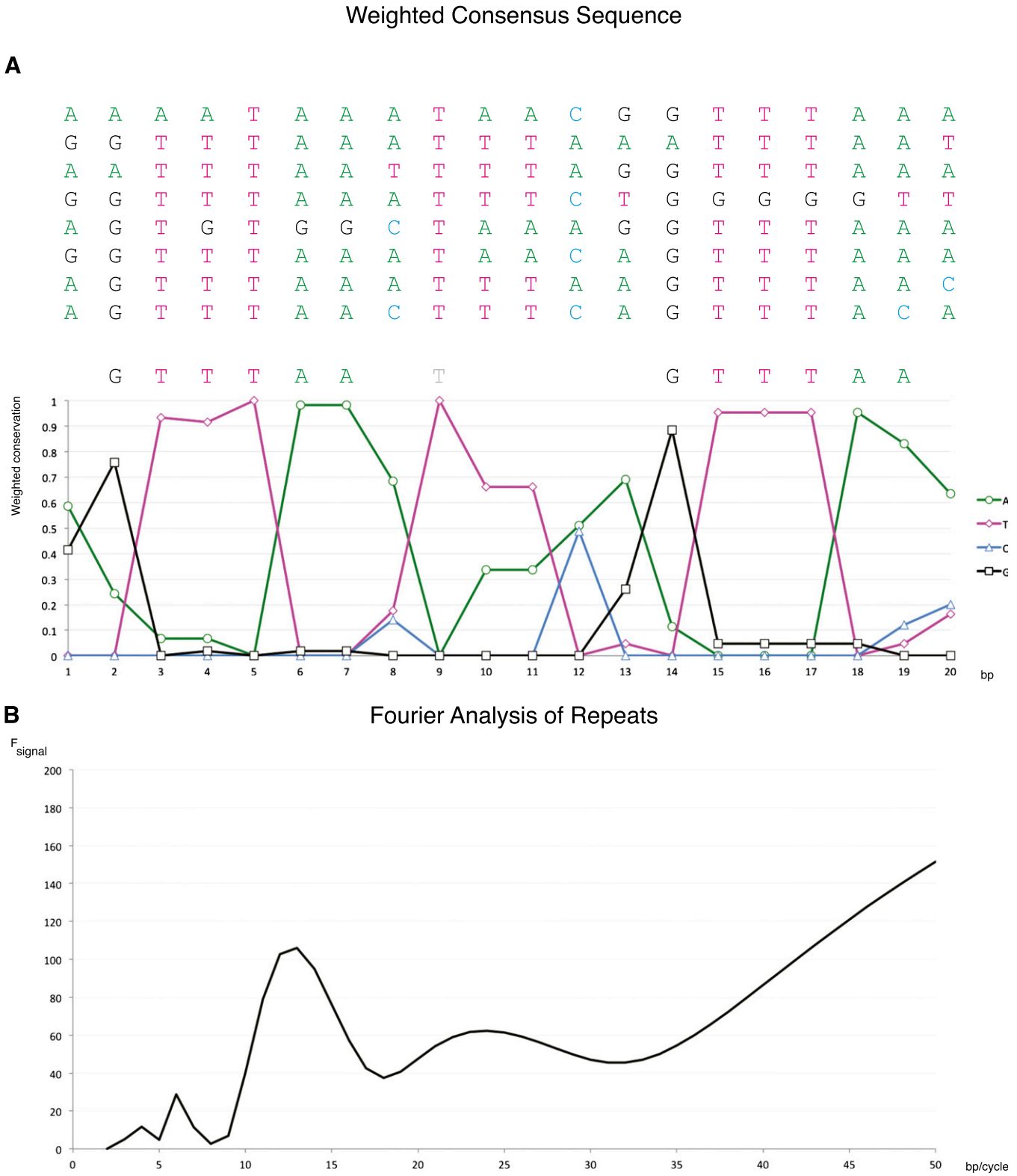

Fig. S1. Assignment of the repeat length and consensus sequence of *Bt* TubR binding sites in *tubC*. (*A*) Aligned sequences of the seven peaks of *Bt* TubR binding and graph of the weighted alignment below (total summing to unity). (*B*) Graph of Fourier magnitudes of *Bt* TubR binding signal against reciprocal base pair repeat, sites 4–7.

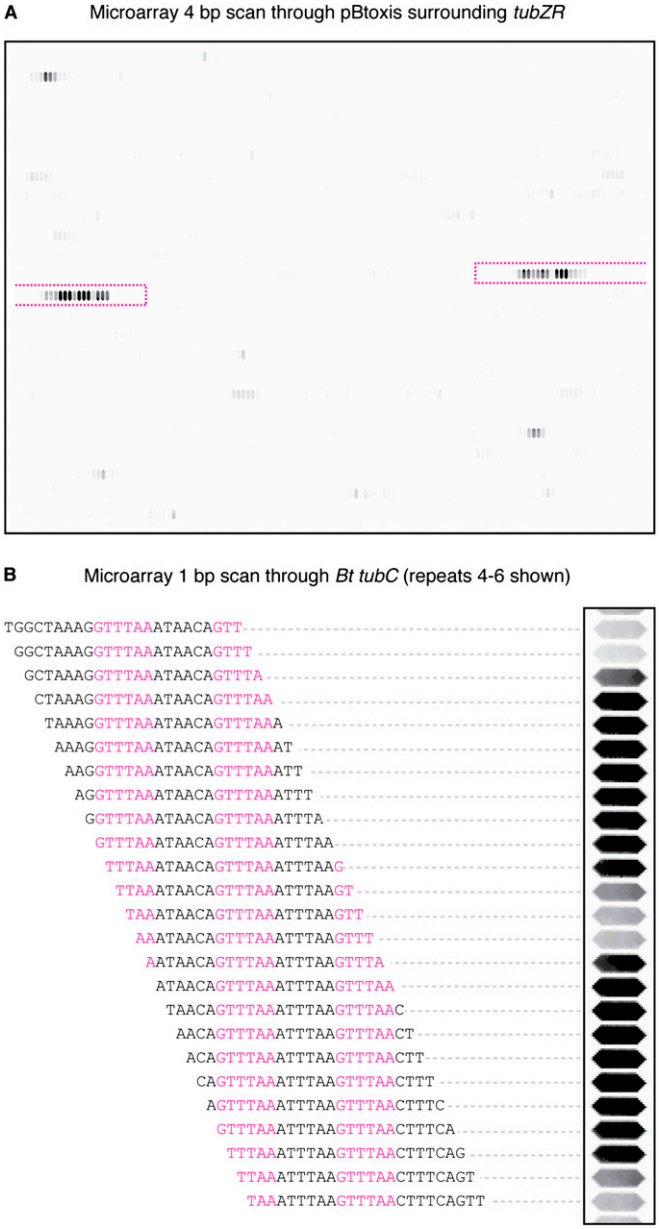

Fig. S2. A *Bt tubC* microarray was probed with TubR. (*A*) An area of the *Bt tubC* microarray showing binding of *Bt* TubR (black) to sequences sampled at 4-bp intervals through pBtoxis (bp 122000 to 3100). The sequence runs from left to right, top to bottom. (*B*) Part of the microarray showing binding of *Bt* TubR (black) to sequences sampled at 1-bp intervals through part of *Bt tubC* (bp 126577 to 126530), the aligned sequences of the hairpins are shown, magenta indicating the consensus site.

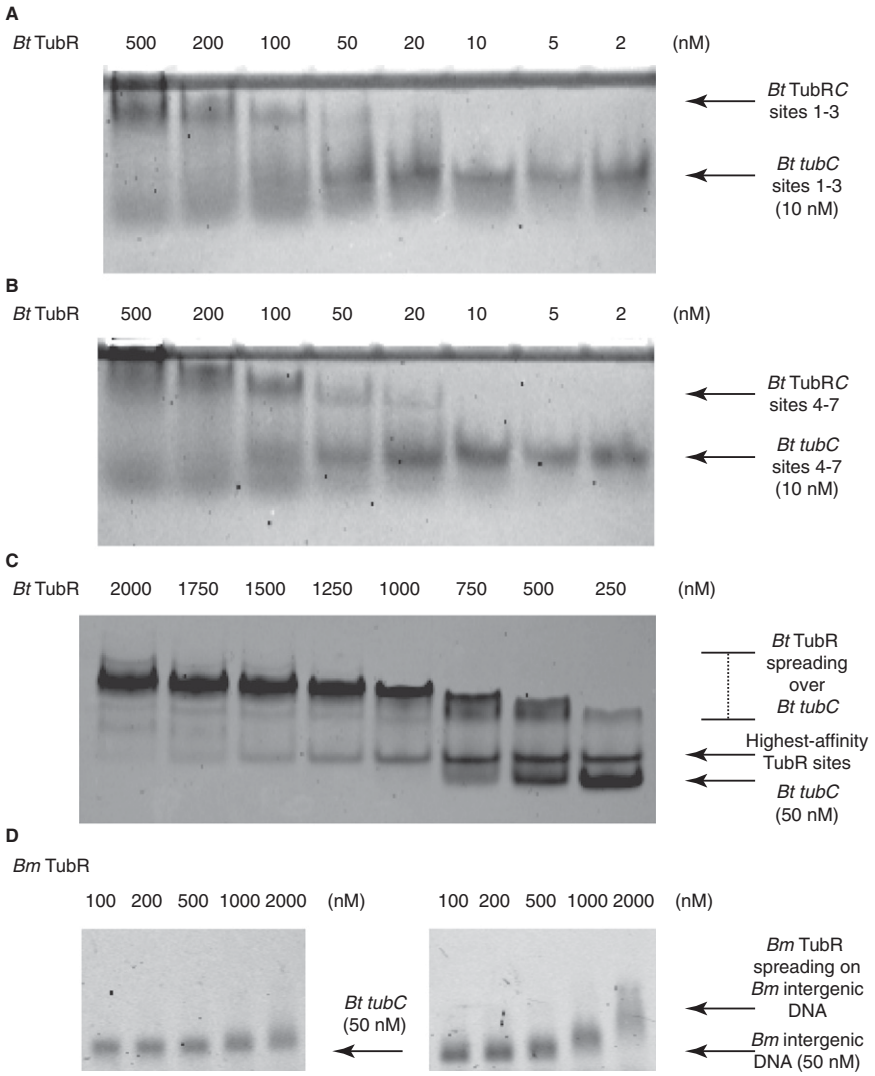

Fig. S3. *Bt* TubR binds cooperatively to both sets of *tubC* repeats. (*A*) Electrophoretic mobility shift assay showing binding by TubR during titration against repeats 1–3 of *tubC*. (*B*) Electrophoretic mobility shift assay showing binding by TubR during titration against repeats 4–7 of *tubC*. (*C*) Electrophoretic mobility shift assay showing binding by TubR during titration against full-length *tubC*. Initial binding to high-affinity sites is visible as a single band slightly above the initial DNA, and the gradual curve thereafter during titration implies lateral spreading by *Bt* TubR. (*D*) Electrophoretic mobility shift assay showing that *Bm* TubR shows a binding preference toward its 5′ intergenic DNA (*Right*), compared with *Bt tubC* DNA (*Left*). All scans show fluorescence from 5′ fluorescein conjugation.

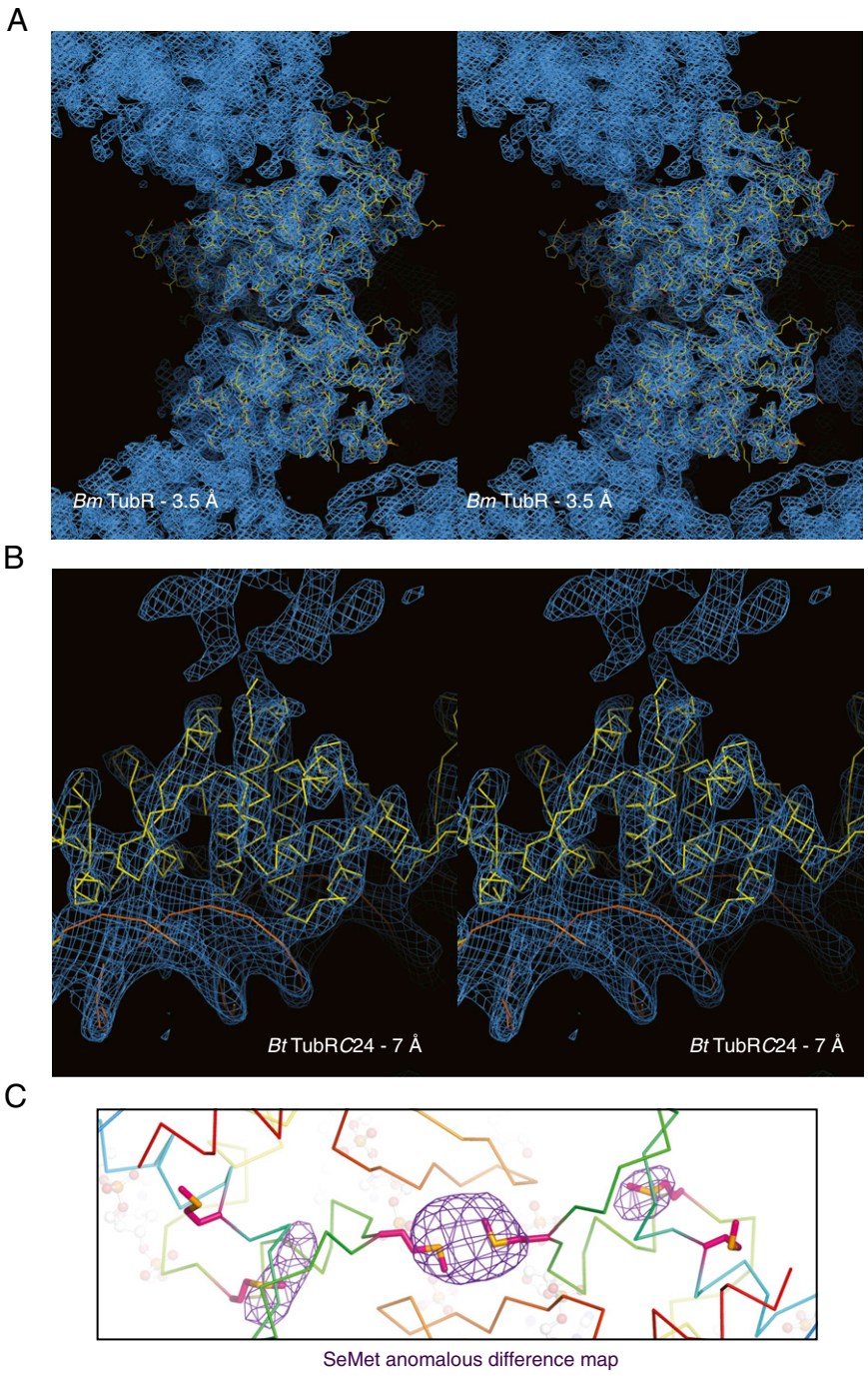

Fig. S4. Electron density from the crystal structures of TubR. (*A*) Stereoscopic images of the structure of *Bm* TubR (density at 1.5 σ in blue, stick representation, C in yellow/CPK colors). (*B*) Stereoscopic images of the structure of *Bt* TubRC24 (density at 1.5 σ in blue, Cα ribbon representation in yellow for protein and brown for DNA). (*C*) Region of the Se anomalous difference map from the structure of *Bt* TubRC24 at 3 σ (purple mesh), Cα ribbon representation, with selenomethionine residues highlighted [stick representation, C in magenta/Corey, Pauling, Koltun (CPK) colors].

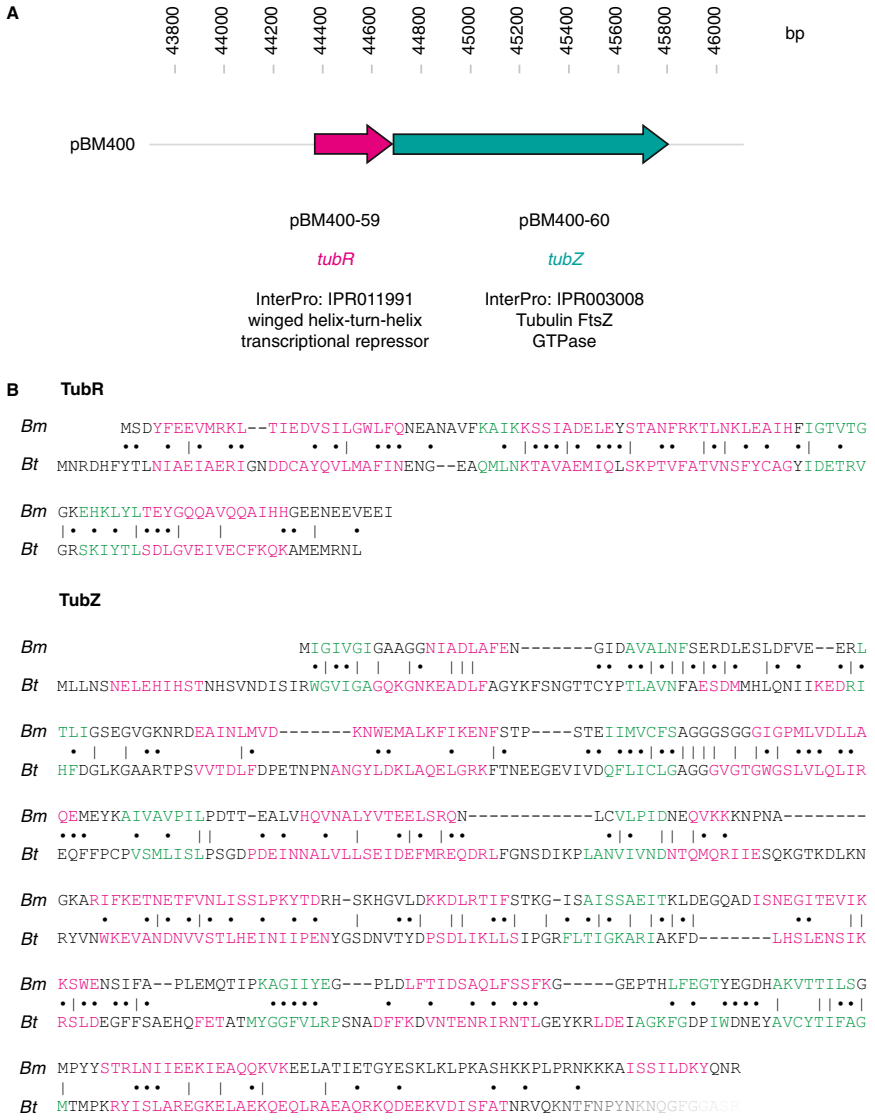

Fig. S5. The *tubZR* operon from *Bacillus megaterium* pBM400. (*A*) Schematic showing the genes *tubR* and *tubZ* in pBM400. InterPro family results (May 2012) are shown to confirm the identity of the two genes. (*B*) Protein sequence alignments of *Bm* TubR and TubZ with *Bt* TubR and TubZ.

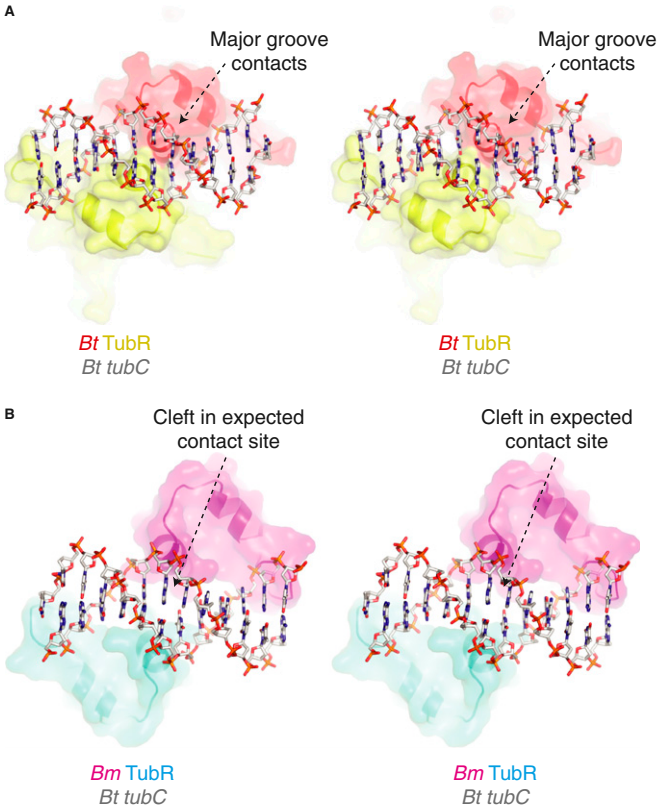

Fig. S6. Superimposition of a *Bm* TubR dimer onto the structure of *Bt* TubRC showing the reduced binding surface within the major groove. (*A*) Stereoscopic image of the structure of one dimer and DNA from *Bt* TubRC (red and yellow, surface representation on cartoon, DNA in CPK colors) showing the major groove contact surface against DNA. (*B*) Stereoscopic image of a structural superimposition of the structure of a *Bm* TubR dimer (cyan and magenta, surface representation on cartoon) onto the Bt TubRC filament (DNA shown only, white and CPK colors) showing the *predicted* major groove contact surface against DNA.

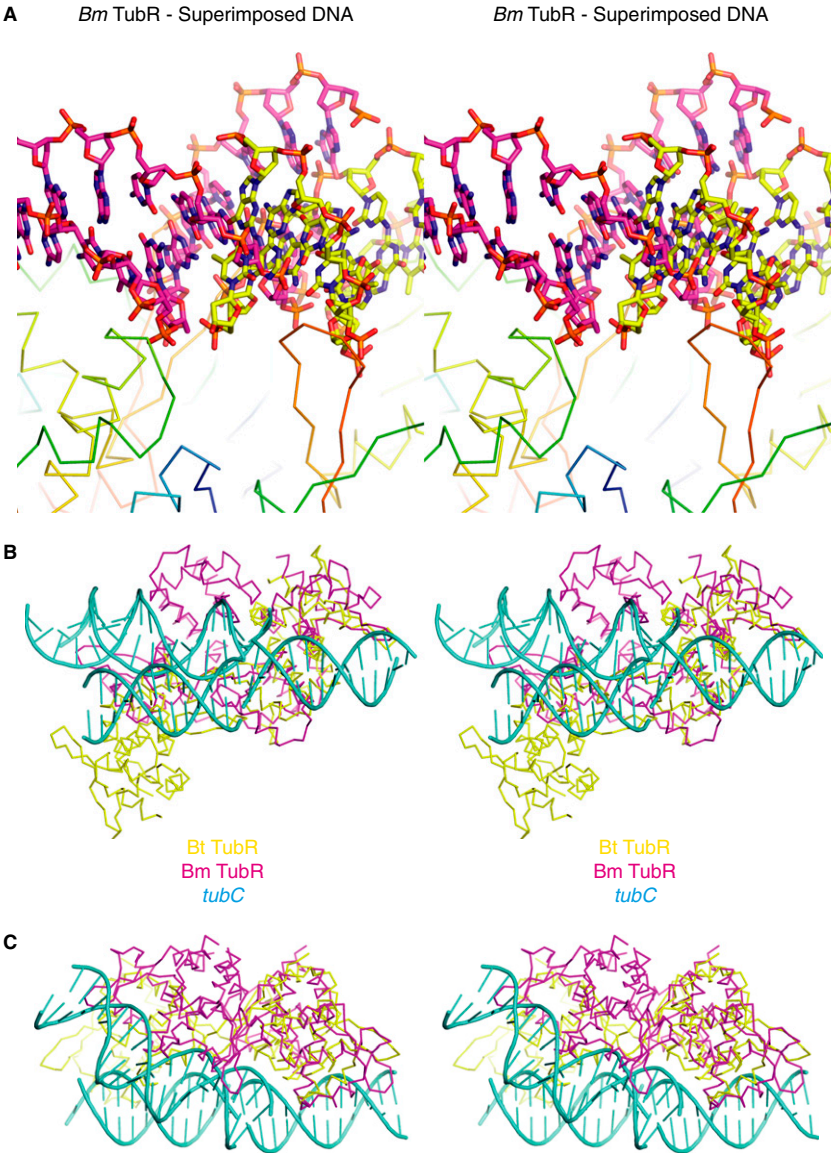

Fig. S7. Two possible modes of binding by TubR to *tubC*. (*A*) Stereoscopic images of the structure of *Bm* TubR (Cα ribbon representation, blue at N terminus, red at C terminus) with DNA (stick representation, C in yellow or magenta/CPK colors) from homologous structure PDB ID code 1HW2 shown after the protein chains have been superimposed. (*B* and *C*) Stereoscopic images of the superimposition of *Bt* TubRC24 (Cα ribbon representation, yellow) and *Bm* TubR (magenta). DNA is shown in cartoon representation, in blue. DNA in the *Bm* TubR form is from PDB ID code 1HW2.

Table S1. Previous experimental results from *Bt* TubR–DNA complexes

Publication	Reference	Experiment	Data/result	Conclusions
Tang et al. (2006)	(1)	Deletion map of this operon	Located *tubZRC* operon	Minireplicon locus (then proposed)
		Sequence analysis of locus	Four repeats (then identified)	*Cis*-acting site in locus DNA
		Gene deletion study	TubR and TubZ were required	Replication genes (then proposed)
Larsen et al. (2007)	(2)	Gene deletion study	TubZ increased if *tubR* deleted	TubR regulates this operon
		Plasmid stability assay	*tubZRC* required for plasmid stability	*tubZRC* plasmid partitioning system
Tang et al. (2007)	(3)	DNA deletion study	DNA repeats necessary	Replication origin (then proposed)
		EMSA of TubR and DNA repeats	TubR binds DNA repeats	TubR is an iteron binding protein
		EMSA of TubR/DNA and TubZ	TubR-DNA binds TubZ	TubR is a regulator of TubZ
Ni et al. (2010)	(4)	Crystallography of TubR in the absence of DNA	TubR structures without DNA at high resolution	Recognition helix dimer/possible DNA binding face
		Mutation of TubR surfaces	Impaired binding to DNA repeats	Dimerization and surfaces required
		Fluorescence polarization of TubR/DNA	TubR titrates to ~8 molecules before inflection	TubR binds ~1 dimer per 12 bp
		Fluorescence polarization of TubR/DNA against TubZ	TubR and DNA interacted with TubZ with H11, but not without	TubZ C terminus required for this interaction

1. Tang M, Bideshi DK, Park HW, Federici BA (2006) Minireplicon from pBtoxis of *Bacillus thuringiensis subsp. israelensis*. *Appl Environ Microbiol* 72:6948–6954.
2. Larsen RA, et al. (2007) Treadmilling of a prokaryotic tubulin-like protein, TubZ, required for plasmid stability in *Bacillus thuringiensis*. *Genes Dev* 21:1340–1352.
3. Tang M, Bideshi DK, Park HW, Federici BA (2007) Iteron-binding ORF157 and FtsZ-like ORF156 proteins encoded by pBtoxis play a role in its replication in *Bacillus thuringiensis subsp. israelensis*. *J Bacteriol* 189:8053–8058.
4. Ni L, Xu W, Kumaraswami M, Schumacher MA (2010) Plasmid protein TubR uses a distinct mode of HTH-DNA binding and recruits the prokaryotic tubulin homolog TubZ to effect DNA partition. *Proc Natl Acad Sci USA* 107:11763–11768.

Table S2. Crystallographic data summary

Statistics	*Bacillus megaterium* TubR	*Bacillus thuringiensis* TubR – *tubC*24
Protein	Full length, untagged	Full length, untagged
UniProt ID no.	Q848W2	Q8KNP2
ATCC ID no.	12872	35646
Collection		
Beamline	ESRF-ID29	Diamond-I03
Wavelength, Å	0.9790	0.9794
Crystal		
Space group	H 3 2	C 1 2 1
Cell, Å	179.9, 179.9, 114.3	519.3, 63.7, 167.3 β = 96.7
Scaling		
Resolution	3.5	7.0
Completeness (%)*	100 (100)	98.1 (98.5)
Multiplicity*	9.9 (10.4)	5.9 (5.9)
Ano completeness (%)*	99.3 (100)	98.1 (97.9)
Ano multiplicity*	4.9 (5.1)	3.2 (3.2)
Ano correlation*,†	0.658 (0.021)	0.858 (0.008)
(I)/σ(I)*,‡	23.1 (4.8)	10.9 (1.3)
R_{merge}*	0.053 (0.431)	0.090 (1.642)
R_{pim}*	0.026 (0.205)	0.052 (0.817)
Phasing		
Scatterer/mode	Se/SAD	Se/MR-SAD
Number of sites	3	
Figure of merit	0.72	
Refinement		
R/R_{free}§	0.1858/0.2284	0.3443/0.3712
Bond length rmsd, Å	0.013	
Bond angle rmsd, °	1.324	
Most favored, %**	86.3	
Disallowed, %**	0	
Deposition		
PDB ID code	4ASN	4ASO

*Values in parentheses refer to the highest recorded resolution shell.
†Anomalous correlation coefficient between half sets (SCALA).
‡Resolution cutoff determined by half-shell correlation coefficient falling below 0.7.
§5% of reflections were randomly selected before refinement.
**Percentage of residues in the Ramachandran plot (PROCHECK).